

THITIPORN SUTTIKUL<sup>1,2</sup>  
 SIRIMAS MANTHUNG<sup>1</sup>  
 SASIKARN NUCHDANG<sup>3</sup>  
 DUSSADEE RATTANAPHRA<sup>3</sup>  
 THONGCHAI PHOTSATHIAN<sup>4</sup>

<sup>1</sup>Division of Chemical Process Engineering Technology, Faculty of Engineering and Technology, King Mongkut's University of Technology North Bangkok, Rayong, Thailand

<sup>2</sup>The Plasma and Automatic Electric Technology Research Group, King Mongkut's University of Technology North Bangkok, Rayong, Thailand

<sup>3</sup>Research and Development Division, Thailand Institute of Nuclear Technology, Pathum Thani, Thailand

<sup>4</sup>Division of Instrumentation and Automation Engineering Technology, Faculty of Engineering and Technology, King Mongkut's University of Technology North Bangkok, Rayong, Thailand

SCIENTIFIC PAPER

UDC 66.094.3:54:533.9

## ONE-STEP CONVERSION OF ETHANE TO ETHYLENE OXIDE IN AC PARALLEL PLATE DIELECTRIC BARRIER DISCHARGE

### Article Highlights

- For the first time, DBD was used to perform a one-step direct conversion of C<sub>2</sub>H<sub>6</sub> to EO
- The effects of the applied voltage, input frequency, and O<sub>2</sub>/C<sub>2</sub>H<sub>6</sub> feed molar ratio were examined
- Higher voltage and lower frequency generated more electrons, resulting in higher current
- The higher activity resulted from more electrons interacting with reactant gas molecules

### Abstract

*This work studied the one-step conversion of ethane (C<sub>2</sub>H<sub>6</sub>) to ethylene oxide (EO) in an AC parallel plate dielectric barrier discharge (DBD) system with two frosted glass plates under ambient temperature and atmospheric pressure. EO is directly produced from C<sub>2</sub>H<sub>6</sub> in a single step without the requirement to separate and recycle ethylene. The effects of the applied voltage, input frequency, and O<sub>2</sub>/C<sub>2</sub>H<sub>6</sub> feed molar ratio on the EO synthesis performance were examined. The results showed that a higher applied voltage and lower input frequency generated more highly energetic electrons, resulting in a higher current. More electrons collided with reactant gas molecules to initiate plasma reactions, increasing C<sub>2</sub>H<sub>6</sub> and O<sub>2</sub> conversions. The increased O<sub>2</sub>/C<sub>2</sub>H<sub>6</sub> feed molar ratio enhanced C<sub>2</sub>H<sub>6</sub> and O<sub>2</sub> conversions. The optimum conditions were found to be an applied voltage of 7 kV, input frequency of 550 Hz, and O<sub>2</sub>/C<sub>2</sub>H<sub>6</sub> feed molar ratio of 1:1, which demonstrated the highest EO selectivity (42.6%), EO yield (19.4%), and lowest power consumption per EO molecule produced (6.7 × 10<sup>-18</sup> Ws/molecule).*

*Keywords: dielectric barrier discharge, epoxidation, ethane oxidative dehydrogenation, ethylene oxide, one-step reaction.*

The manufacture of ethylene oxide (EO) is a rapidly expanding industry in which silver is used as a catalyst. The market for ethylene oxide is expected to

increase at a compound annual growth rate (CAGR) of 4.56% over the forecast period, from US\$48.240 billion in 2019 to US\$65.912 billion in 2026 [1]. Ethylene oxide (C<sub>2</sub>H<sub>4</sub>O, EO) is a versatile chemical that is utilized as a starting material for the production of a variety of beneficial goods. For instance, ethylene glycol, a primary product of EO, is used as a feedstock to synthesize antifreeze and plastics, such as polyethylene terephthalate [2-5]. Surfactant, ethanolamine solvent, and glycol ether solvent were produced by EO alkoxylation processes [5]. In addition, EO is generally used as a sterilizer for medical

Correspondence: T. Suttikul, Division of Chemical Process Engineering Technology, Faculty of Engineering and Technology, King Mongkut's University of Technology North Bangkok, Rayong Campus, Rayong 21120, Thailand.  
 E-mail: thitiporn.s@eat.kmutnb.ac.th  
 Paper received: 28 February, 2023  
 Paper revised: 17 July, 2023  
 Paper accepted: 3 October, 2023

<https://doi.org/10.2298/CICEQ230228026S>

equipment and supplies such as needles, surgical cords, and surgical supplies [6].

Partial oxidation of ethylene ( $C_2H_4$ ), the so-called ethylene epoxidation, commercially produces EO using Ag-based catalysts with promoters (Re, Cs, Mo, Cl, etc.) and provides a considerably high EO selectivity of 80–90% [7–9].  $C_2H_4$  used as a reactant in forming EO, is typically obtained via oxidative dehydrogenation of ethane (ODHE). The exothermic ODHE reaction takes place at temperatures between 673 and 873 K [10], while  $C_2H_4$  epoxidation utilizing Ag/(LSA)  $\alpha$ - $Al_2O_3$  only requires a reaction temperature below 573 K [11]. There have been several attempts to develop a bifunctional catalyst that would enable the direct synthesis of EO from ethane ( $C_2H_6$ ) in a single step without the requirement to separate and recycle  $C_2H_4$ . A NiAgO catalyst directly produced EO from  $C_2H_6$  [12]. After that, a  $Y_2O_3$  promoter was used to improve the properties of the catalyst, particularly its electrophilic nature [13]. For the direct conversion of  $C_2H_6$  to EO, the NiAgYO catalyst demonstrated higher EO selectivity and yield than NiAgO. The interaction between Y and Ag, which caused the absorbed oxygen species to possess proper electrophilic character, led to the enhanced performance of the NiAgYO catalyst. However, the NiAgYO catalyst exhibited low EO selectivity and yield of 19.8% and 7.6%, respectively, at 563 K. Therefore, it is highly desirable to continue the development of an active catalyst and to identify potential innovative, low-temperature operating techniques that can improve reaction performance.

Nonthermal plasma (NTP) is an ionized gas typically produced by an electric discharge [14]. Various reactive species, including vibrationally or electrically activated molecules, radicals, atoms, and ions, are produced when free electrons in the plasma impact gas particles. The major property of NTP is that the temperature of the electrons can be in the range of  $10^4$ – $10^5$  K, while the bulk gas temperature is close to ambient (300–1000 K). Dielectric barrier discharge (DBD) is a type of nonthermal plasma (NTP) that can operate at ambient temperature (nearly 298 K) and atmospheric pressure, resulting in relatively low energy consumption. DBD has received the most attention for plasma-enhanced catalysis, such as the conversion of  $CO_2$  and  $CH_4$  into synthesis gas and value-added liquid chemical [15–17], volatile organic compound decomposition [18–20], remediation of contaminated soil [21–23], and  $C_2H_4$  epoxidation [24–28], which our research team studied. A separate feed of  $C_2H_4$  from  $O_2$  with a suitable  $C_2H_4$  feed position was demonstrated to decrease undesired reactions such as cracking, partial oxidation, and hydrogenation in investigations of DBD, corona discharge, and dielectric barrier

discharge jet (DBDJ) systems [27], as compared to a mixed feed [24]. The DBDJ achieved the highest energy efficiency of 703.65 mmol/kJ (Table 1). However, packing a catalyst in the plasma zone of a DBDJ reactor is cumbersome, and the discharge becomes unstable. In comparison to DBD with an Ag catalyst loaded on a single smooth glass plate [26], it was discovered that the DBD-alone system using two frosted glass plates improved the  $C_2H_4$  epoxidation performance by achieving a reasonably high EO selectivity and yield of 68.2% and 10.9%, respectively [28]. The results are attributable to the fact that frosted glass plates offered more sharp points than smooth glass plates, generating more uniform plasma with a better distribution of energy densities. Pulse corona discharge, a kind of NTP, was used to study the ODHE with carbon dioxide at room temperature and atmospheric pressure over several catalysts [29]. The corona discharge using a Pd/ $\gamma$ - $Al_2O_3$  catalyst had a 46.7%  $C_2H_4$  selectivity and 30.0%  $C_2H_6$  conversion. Non-oxidative ethane dehydrogenation (EDH) was investigated in a packed-bed DBD reactor [30]. As a result,  $C_2H_4$  is the primary byproduct, followed by acetylene ( $C_2H_2$ ), methane ( $CH_4$ ), and  $C_3/C_4$  hydrocarbons. A  $SiO_2$ -supported Pd catalyst can change the product selectivity and distort the electric field. From the literature mentioned above, we hypothesize that DBD can be used for the ODHE reaction to form  $C_2H_4$  and then further convert to EO.

In this study, the one-step conversion of  $C_2H_6$  and  $O_2$  to EO was investigated for the first time in an AC parallel-plate DBD with two frosted glass plates. The effects of various operating parameters, including the applied voltage, input frequency, and  $O_2/C_2H_6$  feed molar ratio, on the EO synthesis performance were experimentally studied to determine the optimum conditions.

## MATERIALS AND METHODS

### Gases for the reaction experiment

In this work,  $C_2H_6$  with a purity of 99.5%, oxygen with a purity of 99.5%, and helium with a purity of 99.995% (high purity grade) were blended to produce a feed gas.  $C_2H_6$  was supplied by Linde (Thailand) Public Co., Ltd., whereas Thai Industrial Gas Co., Ltd. supplied oxygen and helium.

### Setup and reaction testing experiments

The one-step conversion of  $C_2H_6$  to EO was investigated in a parallel-plate DBD reactor at atmospheric pressure and ambient temperature (approximately 298 K). A schematic diagram of the experimental setup is illustrated in Fig. 1, and an

Table 1. Comparison of the catalyst-alone and DBD-alone systems on the EO synthesis performance.

System (conditions)	Conversion (%)			Selectivity (%)		Yield (%)		Power consumption			Energy efficiency (mmol/kJ)
	C <sub>2</sub> H <sub>6</sub>	C <sub>2</sub> H <sub>4</sub>	O <sub>2</sub>	EO	C <sub>2</sub> H <sub>4</sub>	EO	C <sub>2</sub> H <sub>4</sub>	C <sub>2</sub> H <sub>6</sub> converted	C <sub>2</sub> H <sub>4</sub> converted	EO produced	
Parallel DBD using a clear glass plate [24] (Mixed feed, O <sub>2</sub> /C <sub>2</sub> H <sub>6</sub> molar ratio of 1/1, applied voltage of 19 kV, an input frequency of 500 Hz, and a total feed flow rate of 50 cm <sup>3</sup> /min)	-	91.0	93.7	6.2	-	5.6	-	-	4.0 × 10 <sup>-17</sup>	#6.1 × 10 <sup>-16</sup> ~102.0	N/A
Corona discharge [25] (Separate feed [C <sub>2</sub> H <sub>4</sub> feed position of 0.2 cm], O <sub>2</sub> /C <sub>2</sub> H <sub>4</sub> molar ratio of 0.5/1, applied voltage of 18 kV, input frequency of 500 Hz, and total feed flow rate of 100 cm <sup>3</sup> /min)	-	2.3	44.3	78.1	-	1.8	-	-	4.7 × 10 <sup>-18</sup>	#6.1 × 10 <sup>-16</sup> ~1.0	0.02
DBDJ [27] (Separate feed [C <sub>2</sub> H <sub>4</sub> feed position of 0.3 cm], O <sub>2</sub> /C <sub>2</sub> H <sub>4</sub> molar ratio of 0.25/1, applied voltage of 9 kV, input frequency of 500 Hz, and total feed flow rate of 1,625 cm <sup>3</sup> /min)	-	50.0	91.2	55.2	-	27.6	-	-	3.3 × 10 <sup>-21</sup>	#6.0 × 10 <sup>-21</sup> ~1.0 × 10 <sup>-3</sup>	703.65
Parallel DBD using two frosted glass plates [28] (Separate feed [C <sub>2</sub> H <sub>4</sub> feed position of 0.5], O <sub>2</sub> /C <sub>2</sub> H <sub>4</sub> molar ratio of 0.2/1, applied voltage of 23 kV, input frequency of 500 Hz, and total feed flow rate of 50 cm <sup>3</sup> /min)	-	19.8	99.5	68.1	-	10.9	-	-	1.9 × 10 <sup>-16</sup>	#2.8 × 10 <sup>-16</sup> ~46.8	0.03
Catalytic process using Cs-Re15% Ag/ $\alpha$ - Al <sub>2</sub> O <sub>3</sub> [40] (Reaction temperature of 499K, O <sub>2</sub> /C <sub>2</sub> H <sub>4</sub> molar ratio of 0.25/1, space velocity of 5,000 h <sup>-1</sup> )	-	10.0	N/A	83.5%	-	N/A	-	-	N/A	N/A	N/A
Catalytic process using 0.32% Sn-1.39% Cu-17.16% Ag/SrTiO <sub>3</sub> [41] (Reaction temperature of 548K, O <sub>2</sub> /C <sub>2</sub> H <sub>4</sub> molar ratio of 1/1, space velocity of 6,000 h <sup>-1</sup> )	-	5.4	N/A	99.2	-	5.4	-	-	N/A	N/A	N/A
Parallel DBD using two frosted glass plates (This work) (Mixed feed, O <sub>2</sub> /C <sub>2</sub> H <sub>6</sub> molar ratio of 1/1, applied voltage of 7 kV, an input frequency of 550 Hz, and a total feed flow rate of 50 cm <sup>3</sup> /min)	45.3	-	99.2	42.6	-	19.4	-	2.9 × 10 <sup>-18</sup>	-	#6.7 × 10 <sup>-18</sup> ~1.1	0.73
Cylindrical DBD using unloaded SiO <sub>2</sub> catalyst [30] (Mixed feed, 5% C <sub>2</sub> H <sub>6</sub> in helium, applied voltage of 10 kV, and a total feed flow rate of 60 cm <sup>3</sup> /min)	~20	-	-	-	~26	-	~3.8	N/A	-	-	0.13
Catalytic process using 5% Ni-Ag-O [12] (Reaction temperature of 583K, O <sub>2</sub> /C <sub>2</sub> H <sub>6</sub> molar ratio of 1/1, gaseous hourly space velocity of 24,000 mLh <sup>-1</sup> g <sup>-1</sup> )	9.3	-	N/A	12.8	-	1.2	-	N/A	-	N/A	N/A
Catalytic process using 5% NiAgYO [13] (Reaction temperature of 563K, O <sub>2</sub> /C <sub>2</sub> H <sub>6</sub> molar ratio of 1/1, gaseous hourly space velocity of 12,000 mLh <sup>-1</sup> g <sup>-1</sup> )	38.4	-	N/A	19.8	-	7.6	-	N/A	-	N/A	N/A

Unit of power consumption; peak marked with *hash* corresponds to Ws/EO molecule produced, with an *asterisk* to kWh per mol of EO.

explanation of the DBD reactor can be found in our previous work [28]. The 2 mm frosted glass plate was washed with distilled water and then cleaned with acetone before use as a dielectric material in the DBD reactor. A microdischarge was produced at a distance of 3 mm between the two parallel frosted glass plates by a specially designed AC power supply. The domestic AC electricity (220 V and 50 Hz) was transformed using three steps to a high-voltage AC (applied voltage of 1–25 kV), according to our prior study [31]. A digital power analyzer (True RMS Single Phase Power Analyzer, 380801, Exttech Instruments

Corporation) was used to monitor input current and power. The power analyzer digitalized the incoming voltage and current waveforms, which then used the voltage and current product over time to calculate the plasma power. A function generator drove the power supply to obtain desired frequency and voltage ranges of 300–800 Hz and 5–11 kV. The temperature was measured using a type K thermocouple with an Agilent U1273A digital multimeter. The temperature of the outside surface of the DBD reactor was kept at  $298 \pm 1$  K by air cooling. The exit gas temperature was  $298 \pm 0.5$  K for all experiments.

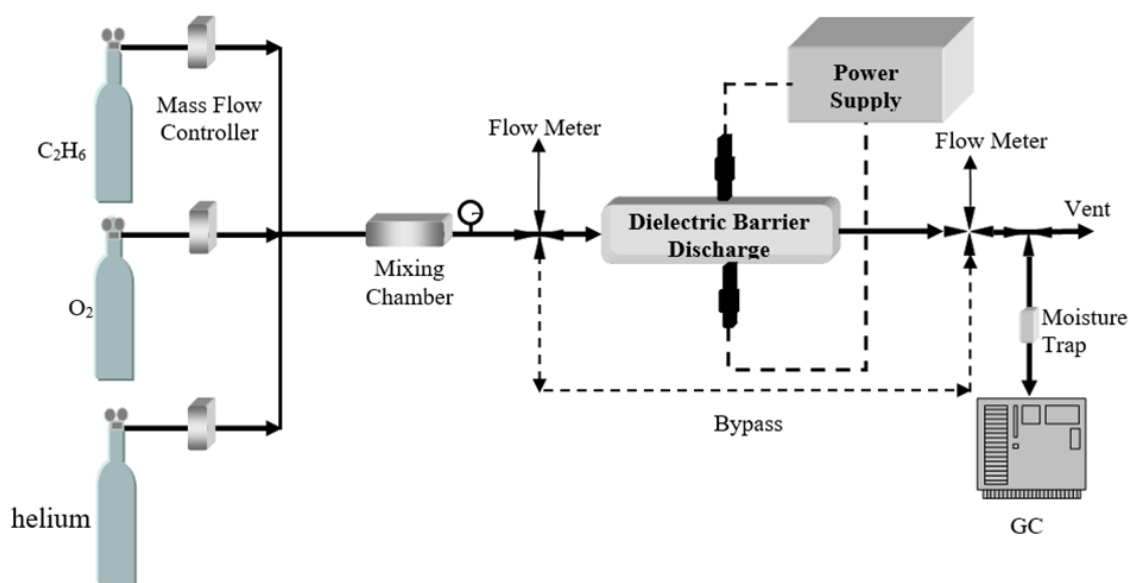


Figure 1. Schematic diagram of the experimental setup of the DBD system for EO production.

For plasma reaction testing, the reactant gases ( $C_2H_6$  and  $O_2$ ) were mixed with helium as a balancing gas to obtain a total flow rate of  $50 \text{ cm}^3/\text{min}$  and an  $O_2/C_2H_6$  molar ratio of 0.5:1. All gases were fed into the DBD reactor using electronic mass flow controllers (AALBORG Instruments & Controls, USA). After the AC power supply was turned on to initiate the plasma reactions, the composition of the effluent gas was analyzed by online gas chromatography (GC, PerkinElmer Clarus 590, USA) with a flame ionization detector (FID) and thermal conductivity detector (TCD) every 20 minutes and at least three times for each reaction. The composition of the hydrocarbon (HC) molecules, such as  $CH_4$ ,  $C_2H_2$ ,  $C_2H_4$ ,  $C_2H_6$ , propene ( $C_3H_6$ ), propane ( $C_3H_8$ ), butane ( $C_4H_{10}$ ), and EO, was determined using an FID detector outfitted with a PorapLOT U column. The composition of the nonhydrocarbon molecules, including hydrogen ( $H_2$ ),  $O_2$ , carbon monoxide (CO), and carbon dioxide ( $CO_2$ ), was evaluated using a TCD detector fitted with a Shin Carbon ST column.

Each reaction was carried out three times. The

average data with less than 5% variation were used to compute the  $C_2H_6$  and  $O_2$  conversions, the selectivity towards EO,  $H_2$ , CO,  $CH_4$ ,  $C_2H_2$ ,  $C_2H_4$ ,  $C_3H_8$ , and  $C_4H_{10}$ , the EO yield, and the amount of coke formation using the following equations:

$$\text{Reactant conversion (\%)} = \frac{(M_{in} - M_{out})}{M_{in}} \cdot 100\% \quad (1)$$

$$\text{Product selectivity (\%)} = \frac{C_P P}{\sum (C_R R)} \cdot 100\% \quad (2)$$

$$H_2 \text{ selectivity (\%)} = \frac{H_P P}{H_R R} \cdot 100\% \quad (3)$$

$$\text{EO yield (\%)} = \frac{C_2H_6 \text{ conversion (\%)} \cdot \text{EO selectivity (\%)}}{100} \quad (4)$$

$$\text{Coke (\%)} = \frac{\sum (C_R R)_{input} - \sum (C_R R + C_P P)_{output}}{\sum (C_R R)_{input}} \cdot 100\% \quad (5)$$

where  $M_{in}$  is the moles of reactant in the input,  $M_{out}$  is the moles of reactant in the output,  $C_R$  is the number of carbon atoms in the reactant,  $R$  is the moles of reactant converted,  $C_P$  is the number of carbon atoms in the product,  $P$  is the moles of product produced,  $H_R$  is the

number of hydrogen atoms in the reactant ( $C_2H_6$ ), and  $H_p$  is the number of hydrogen atoms in the product ( $H_2$ ).

Eqs. (6) and (7) were used to calculate power consumption in a unit of Ws per  $C_2H_6$  molecule converted or per EO molecule produced and energy efficiency in a unit of mmol/kJ used, respectively.

$$\text{Power consumption} = \frac{\text{Power (W)} \cdot 60}{A \cdot M} \quad (6)$$

$$\text{Energy efficiency} \left( \frac{\text{mmol}}{\text{kJ}} \right) = \frac{\text{Rate of reactant converted} \left( \frac{\text{mol}}{\text{min}} \right) \cdot 10^6}{\text{Power (W)} \cdot 60} \quad (7)$$

where  $A$  is Avogadro's number ( $6.022 \times 10^{23}$  molecules/mol), and  $M$  is the rate of  $C_2H_6$  molecules converted in feed or the rate of EO molecules produced (mol/min).

## RESULTS AND DISCUSSION

### Possible chemical reactions

The following equations represent possible chemical pathways in the DBD reactor used in this study. First, high-energy electrons cracked  $O_2$  into active oxygen species (Eq. 8). The active oxygen species then reacted with  $C_2H_6$  to form  $C_2H_4$  and water, a process known as oxidative dehydrogenation of  $C_2H_6$  Eq. (9). As expected,  $C_2H_4$  epoxidation produced the desired EO (Eq. 10).

$O_2$  dissociation [32]:



Oxidative dehydrogenation of  $C_2H_6$  [33]:

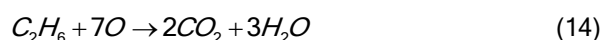
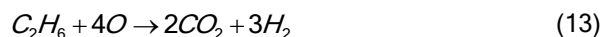


$C_2H_4$  epoxidation [28]:



In addition to EO and  $C_2H_4$ ,  $CH_4$ ,  $CO$ ,  $C_3H_8$ , and  $H_2$  were also produced from plasma reactions. The partial and complete oxidation reactions created  $CO$ ,  $CO_2$ ,  $H_2$ , and  $H_2O$  molecules (Eqs. 11–14). The GC analysis revealed no  $CO_2$  peak (low amount until it could not be detected), which could be because high energy electrons cracked  $CO_2$  into  $CO$  and oxygen species (Eq. 15). The  $CH_4$  and  $C_3H_8$  molecules could be formed by cracking reactions, as shown in Eqs. (16–19), followed by hydrocarbon free radical coupling reactions (Eqs. 20–23).

Partial and complete oxidation [34]:



Cracking [28, 32, 35, 36]:



Coupling [35–37]:



### Effect of applied voltage

The direct conversion of  $C_2H_6$  to EO was investigated in the DBD reactor using two frosted glass plates under atmospheric pressure and ambient temperature ( $\sim 298$  K) without the requirement of other external heat sources. Figure 2 shows the influence of the applied voltage on the reaction performance regarding the  $C_2H_6$  and  $O_2$  conversions, current, EO selectivity and yield, other product selectivities, and power consumption. The applied voltage was investigated in the 5–11 kV range, while an input frequency of 500 Hz, flow rate of 50  $cm^3/min$ , and  $O_2/C_2H_6$  feed molar ratio of 0.5:1 were fixed. As shown in Fig. 2a, the  $C_2H_6$  conversion significantly increases from 23.3 to 39.7% with increasing applied voltage from 5 to 11 kV. When the applied voltage was increased from 5 to 7 kV, the  $O_2$  conversion considerably increased from 58.4 to 96.9%. Then,  $O_2$  conversion gradually increased to 98.4% as the applied voltage increased to 11 kV. The generated discharge became unstable at applied voltages greater than 11 kV, so the DBD reactor voltages increased to 11 kV. Plasma could not be generated when the applied voltage was less than 5 kV. The  $C_2H_6$  conversion was significantly lower than the  $O_2$  conversion since the DBD system was operated under oxygen-lean conditions with a feed molar ratio of  $O_2/C_2H_6$  of 0.5:1. For complete oxidation, the theoretical molar ratio of  $O_2/C_2H_6$  is 3.5:1. A higher current resulted from a greater number of excited electrons being produced by the higher applied voltage

(Fig. 2a). As a result, increases in the  $C_2H_6$  and  $O_2$  conversions were observed.

As shown in Fig. 2b, the EO selectivity and yield increase, reach the highest values at 7 kV, and decrease with increasing applied voltage over 7 kV. It is interesting to note that one of the primary products of the plasma reactions was  $CH_4$ . Product selectivities were arranged as follows:  $CH_4 > EO > C_2H_4 > CO \gg C_3H_8 > H_2$  (Fig. 2c). The results indicated that the cracking reactions (Eqs. 16–18), followed by the hydrogenation reactions (Eqs. 20–21), into  $CH_4$ , were certainly promoted in the studied DBD system. The selectivities towards  $CH_4$  and  $H_2$  are drastically enhanced over the entire applied voltage range of 5–11 kV, as illustrated in Fig. 2c. A higher applied voltage resulted in a greater number of excited electrons, which increased  $C_2H_6$  and  $O_2$  conversions, and the selectivities towards EO,  $CH_4$ , and  $H_2$  (Fig. 2a and 2b). When the applied voltage exceeded 7 kV, excess excited electrons could crack more  $C_2H_6$  and  $C_2H_4$  molecules, forming lower molecules such as  $CH_4$  and  $H_2$  instead of the desired EO. As a result, the EO selectivity above 7 kV decreased, but the selectivities towards  $CH_4$  and  $H_2$  increased continuously. The  $C_2H_4$  selectivity, on the other hand, tended to considerably decrease as the applied voltage was increased from 5 to 11 kV. At an applied voltage of 7 kV, the  $C_3H_8$  selectivity increased to its maximum level, mirroring the EO selectivity. The CO selectivity increased with

increasing applied voltage, except for the greatest voltage of 11 kV. It could be because the highest applied voltage of 11 kV generated highly energetic electrons that possibly decomposed hydrocarbons into coke and hydrogen and additionally cracked the produced CO into coke and oxygen species in the studied DBD, as follows [38,39]:



Figure 2d illustrates the power consumption used to convert  $C_2H_6$  and to yield EO as a function of applied voltage. A higher applied voltage consumed more power (data not represented here) and produced more highly energetic electrons, which led to a higher current (Fig. 2a). As a result, more electrons collided with reactant gas molecules to initiate plasma reactions, giving rise to more  $C_2H_6$  molecules being converted and EO molecules being produced. As shown in Fig. 2d, the power consumption per  $C_2H_6$  molecule converted increased slightly with increasing applied voltage, while the applied voltage of 7 kV exhibited the highest energy efficiency in terms of the minimum power consumption per EO molecule produced. The results showed that the applied voltage of 7 kV was optimum for the maximum EO production in the studied DBD system because of the highest EO selectivity and EO yield and lowest power consumption per EO molecule produced.

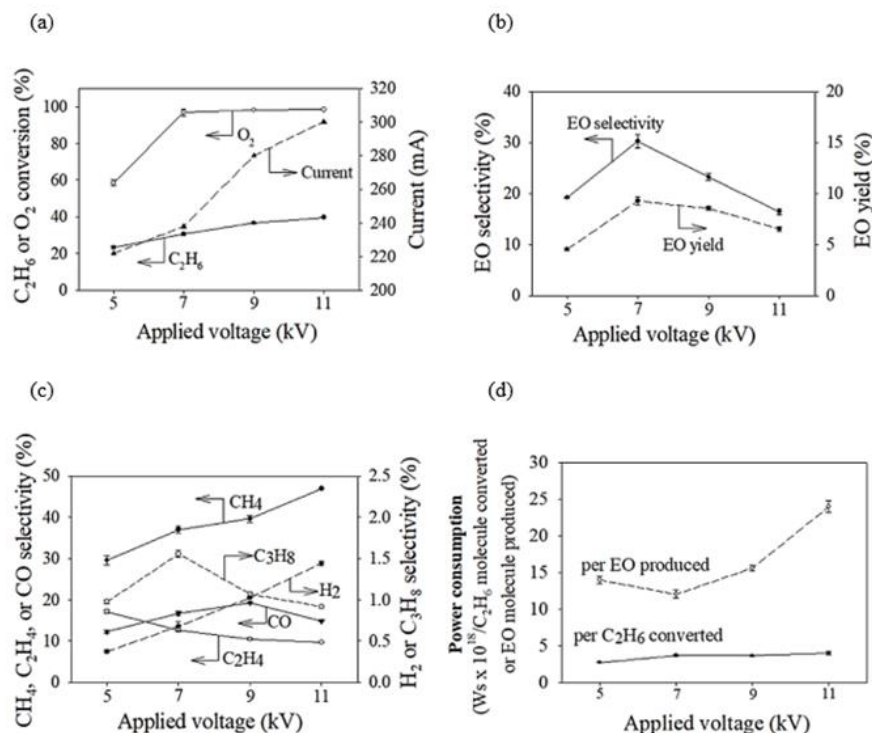


Figure 2. Effect of the applied voltage on (a)  $C_2H_6$  and  $O_2$  conversions and current, (b) EO selectivity and yield, (c) other product selectivities, and (d) power consumption. (Input frequency of 500 Hz, flow rate of  $50 \text{ cm}^3/\text{min}$ , and  $O_2/C_2H_6$  feed molar ratio of 0.5:1).

### Effect of the input frequency

The effect of input frequency on the plasma reaction performance was examined by changing the input frequency from 450 to 600 Hz, while the applied voltage,  $O_2/C_2H_6$  feed molar ratio, and total feed flow rate were maintained at 7 kV, 0.5:1, and 50  $cm^3/min$ , respectively. At input frequencies below 450 Hz, the studied plasma processes produced unreasonably low EO selectivity (less than 5%, data not shown), whereas those over 600 Hz produced unstable plasma. As shown in Fig. 3a, an increased applied voltage from 450 to 550 Hz enhanced the  $C_2H_6$  and  $O_2$  conversions from 13.0% and 61.1% to 32.4% and 98.2%, respectively. Afterward, they rapidly decreased with further increasing applied voltage over 550 Hz.

Both EO selectivity and yield increased with increasing input frequency and reached maximum levels at the same input frequency of 550 Hz, mirroring both  $C_2H_6$  and  $O_2$  conversions (Fig. 3b). As the input frequency increased from 450 to 500 Hz, the selectivities towards  $CH_4$ ,  $C_2H_4$ ,  $C_3H_8$ , and  $H_2$  increased; however, as the input frequency ascended above 500 Hz, the selectivities towards these products declined (Fig. 3c). Interestingly, only the CO selectivity had a similar tendency as the current in that it decreased noticeably with increasing input frequency. The results can be attributed to an increase in current with a reduction in input frequency (Fig. 3a), which

produced more excited electrons and promoted all plasma processes. The selectivities towards EO,  $CH_4$ ,  $C_2H_4$ ,  $C_3H_8$ ,  $H_2$ , and CO dramatically increased with a decrease in input frequency from 600 Hz to 550 Hz (for EO) or 500 Hz (for the others). When the input frequency was lower than 550 Hz, more excited electrons collided with  $O_2$  molecules, resulting in more active oxygen species and further oxidation of EO to CO (Eq. 26). At the lowest input frequency of 450 Hz, excited electrons could collide with  $C_2H_6$  molecules to form hydrocarbons ( $C_2H_5$ ,  $CH_3$ , and  $CH_2$ ) and hydrogen free radicals by cracking reactions (Eqs. 16–19). Instead of producing  $CH_4$  and  $C_3H_8$  molecules (Eqs. 20–22),  $C_2H_5$  free radicals could recombine to produce  $C_2H_6$  molecules (Eq. 27), resulting in lower  $C_2H_6$  conversions. Additionally, the  $CH_3$  and  $CH_2$  free radicals could combine to form  $C_2H_4$  molecules (Eq. 28), which were then further oxidized to produce CO and  $H_2O$  (Eq. 29).

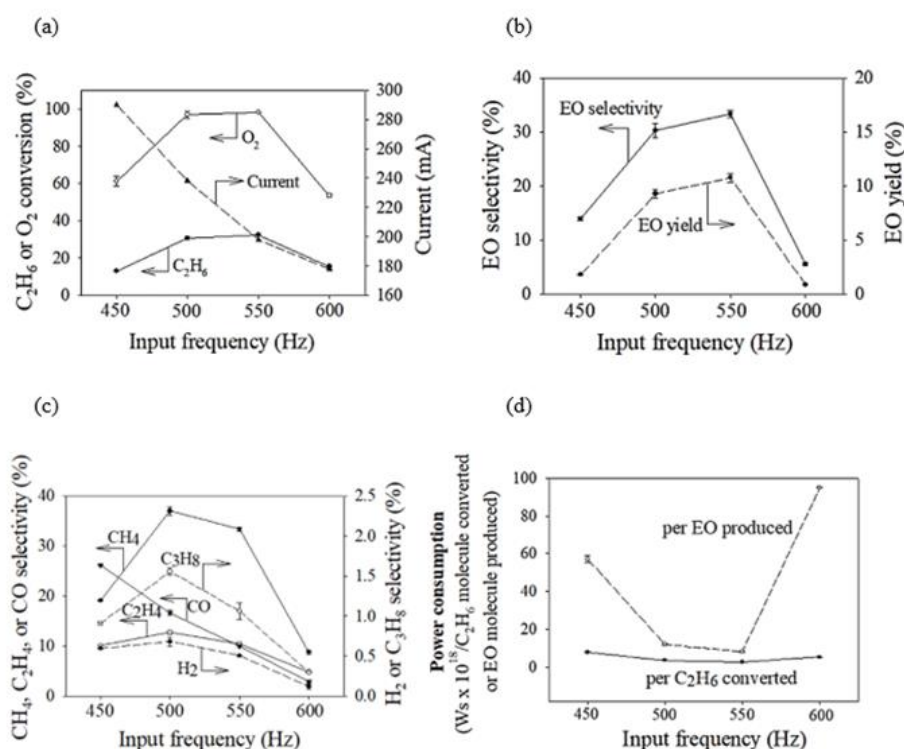
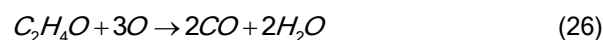


Figure 3. Effect of the input frequency on (a)  $C_2H_6$  and  $O_2$  conversions and current, (b) EO selectivity and yield, (c) other product selectivities, and (d) power consumption. (Applied voltage of 7 kV, flow rate of 50  $cm^3/min$ , and  $O_2/C_2H_6$  feed molar ratio of 0.5:1).

As shown in Fig. 3d, both the power consumption per  $C_2H_6$  molecule converted and per EO molecule produced tend to decrease with increasing input frequency to 550 Hz, which gives the highest  $C_2H_6$  conversion and EO selectivity. The optimal input frequency of 550 Hz was chosen for a subsequent experiment because it provided the greatest  $C_2H_6$  and  $O_2$  conversions, EO selectivity and yield, and lowest power consumption.

### Effect of the $O_2/C_2H_6$ feed molar ratio

The  $O_2/C_2H_6$  feed molar ratio has a significant influence on the process performance of the investigated DBD, as shown in Fig. 4. The  $O_2/C_2H_6$  feed molar ratio was studied in the range of 0.5:1 to 1.25:1 under constant operating conditions, including an applied voltage of 7 kV, input frequency of 500 Hz, and flow rate of  $50\text{ cm}^3/\text{min}$ . The  $C_2H_6$  conversion increased significantly from 32.4 to 48.2%. The  $O_2$  conversion increased slightly from 98.2 to 99.2% when the  $O_2/C_2H_6$  feed molar ratio increased from 0.5:1 to 1.25:1 (Fig. 4a). The DBD system was operated in oxygen lean conditions, which resulted in low  $C_2H_4$  conversion (32.4–48.2%) and high  $O_2$  conversion ( $> 98\%$ ).

The EO selectivity and yield increased with increasing  $O_2/C_2H_6$  feed molar ratio from 0.5:1 and reached maximum values at an  $O_2/C_2H_6$  feed molar ratio of 1:1 (Fig. 4b). However, they adversely

diminished with further increases in the  $O_2/C_2H_6$  feed molar ratio beyond 1:1. As shown in Fig. 4c, the  $CH_4$  selectivity increases with an increase in the  $O_2/C_2H_6$  feed molar ratio from 0.5:1 to 1.25:1, but the  $C_3H_8$  and CO selectivities decline. The  $H_2$  selectivity was slightly changed in the range of 0.5–1.9%, whereas the  $C_2H_4$  selectivity tended to decrease when the  $O_2/C_2H_6$  feed molar ratio was 1:1. At  $O_2/C_2H_6$  feed molar ratios beyond 1:1, the  $C_2H_4$  selectivity was gradually enhanced. Interestingly, the  $C_2H_4$  selectivity trended opposite to the EO selectivity. It could result from the formation of EO from  $C_2H_4$ , an intermediate in the oxidative dehydrogenation of ethane. The higher the  $O_2/C_2H_6$  feed molar ratio is, the more oxygen species are available to initiate  $C_2H_6$  oxidative dehydrogenation (Eq. 9) and  $C_2H_4$  epoxidation (Eq. 10), increasing EO selectivity and yield. However, the partial and total oxidation reactions (Eqs. 11–14) were minimized as a consequence of this study's investigation of oxygen-lean settings. The coke formation, as determined by a carbon balance, tended to increase from 3.9 to 5.5% (data not shown) when the  $O_2/C_2H_6$  feed molar ratio was enhanced from 0.5:1 to 1.25:1. The results indicated that the higher oxygen content resulted in the possibility for further EO oxidation to CO (Eq. 26), and the formed CO might break into coke and oxygen species (Eq. 25) at an  $O_2/C_2H_6$  feed molar ratio over 1:1.

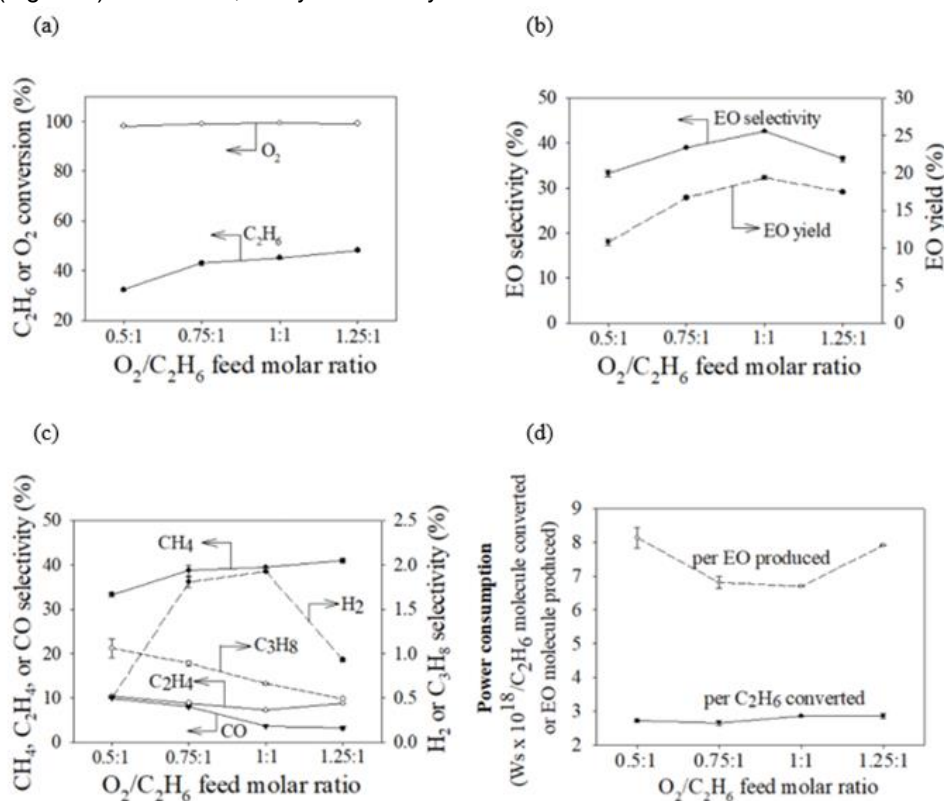


Figure 4. Effect of the  $O_2/C_2H_6$  feed molar ratio on (a)  $C_2H_6$  and  $O_2$  conversions and current, (b) EO selectivity and yield, (c) other product selectivities, and (d) power consumption. (Applied voltage of 7 kV, input frequency of 550 Hz, and flow rate of  $50\text{ cm}^3/\text{min}$ ).



Figure 4d illustrates the power consumption required to convert C<sub>2</sub>H<sub>6</sub> and to produce EO as a function of the O<sub>2</sub>/C<sub>2</sub>H<sub>6</sub> feed molar ratio. The power consumption per C<sub>2</sub>H<sub>6</sub> molecule converted tended to gradually increase as the O<sub>2</sub>/C<sub>2</sub>H<sub>6</sub> feed molar ratio increased to 1.25:1. On the other hand, the power consumption per EO molecule produced decreased considerably and reached a minimum level at an O<sub>2</sub>/C<sub>2</sub>H<sub>6</sub> feed molar ratio of 1:1. From all the results, the optimum O<sub>2</sub>/C<sub>2</sub>H<sub>6</sub> feed molar ratio was 1:1 for maximizing EO production in the DBD system, which exhibited the highest EO selectivity (42.6%) and EO yield (19.4%) and lowest power consumption per EO molecule produced (6.7 x 10<sup>-18</sup> Ws/molecule).

#### Comparisons of the catalyst-alone and different DBD-alone systems on the EO production performance

Ag-based catalysts loaded on various supports, such as Al<sub>2</sub>O<sub>3</sub> and SrTiO<sub>3</sub>, have long been known for their unique ability to selectively oxidize C<sub>2</sub>H<sub>4</sub> to EO in an oxygen atmosphere. Table 1 compares three catalyst-alone and two DBD-alone systems under their optimum conditions. The Cs-Re15% Ag/α-Al<sub>2</sub>O<sub>3</sub> catalyst was used in a catalyst-alone system to provide an outstanding C<sub>2</sub>H<sub>4</sub> epoxidation performance regarding the EO selectivity of 83.5% [40]. Additionally, the catalyst-alone system with the following composition: 0.32% Sn, 1.39% Cu, and 17.16% Ag/SrTiO<sub>3</sub> exhibited an extremely high EO selectivity of 99.2% [41]. On the other hand, both studies reported low C<sub>2</sub>H<sub>4</sub> conversions of 10.0% (for Cs-Re15% Ag) and 5.4% (for 0.32% Sn, 1.39% Cu, 17.16% Ag/SrTiO<sub>3</sub>). In comparison to catalyst-alone systems, the DBD-alone system with two frosted glass plates considerably improves the C<sub>2</sub>H<sub>4</sub> conversion (19.8%) and EO yield (10.9%) while maintaining a reasonably high EO selectivity (68.1%) [28]. According to the findings of this study, the DBD-alone system using a C<sub>2</sub>H<sub>6</sub> reactant resulted in the highest EO yield of 19.4% and a moderately high EO selectivity of 42.6%. Interestingly, the EO selectivity, EO yield, and C<sub>2</sub>H<sub>6</sub> conversion of the DBD-alone system were obviously higher than those of the catalyst-alone system using 5% Ni-Ag-O (EO selectivity of 12.8%, EO yield of 1.2%, and C<sub>2</sub>H<sub>6</sub> conversion of 9.3%) [12] and NiAgYO (EO selectivity of 19.8%, EO yield of 7.6%, and C<sub>2</sub>H<sub>6</sub> conversion of 38.4%) [13]. As previously indicated, when compared to the 5% Ni-Ag-O system, the DBD-alone system's ability to function at room temperature (303 K) without the use of an external heat source allowed it to reduce further oxidation to CO<sub>x</sub>, increasing EO selectivity and yield. The lower the applied voltage in the studied DBD system, the lower the consumed power. On the other hand, the higher the input frequency is, the lower the consumed power. As a result, the DBD used in this work required less power consumption per EO

produced (6.7×10<sup>-18</sup> Ws/EO molecule produced, equivalent to 1.1 kWh/mole of EO) than the DBD used in the prior work (2.8 × 10<sup>-16</sup> Ws/EO molecule produced, equivalent to 46.8 kWh/mole of EO) [28]. The EDH carried out in the cylindrical DBD using an unloaded SiO<sub>2</sub> catalyst [30] and the C<sub>2</sub>H<sub>4</sub> epoxidation accomplished in the parallel DBD using two frosted glass plates [28] are examples of the two-step pathway. Table 1 demonstrates that the one-step approach had a higher energy efficiency (0.73 mmol/kJ) than the two-step pathway (0.13 mmol/kJ for the EDH and 0.03 for the C<sub>2</sub>H<sub>4</sub> epoxidation). Interestingly, the power consumption of the one-step approach (1.1 kWh/ mole of EO) was extremely lower than that of the two-step pathway (48.0 kWh/ mole of EO). It demonstrated the benefits of the one-step technique, including its lower cost of materials (C<sub>2</sub>H<sub>6</sub> vs. C<sub>2</sub>H<sub>4</sub>), improved energy efficiency, and lower power consumption requirements. Although the present study's results indicate reasonably high EO production performance and low power consumption, it is still necessary to increase EO selectivity. It will be done in a further study by combining a DBD system with efficient catalysts, such as Ni to enhance the possibility of C<sub>2</sub>H<sub>6</sub> oxidative dehydrogenation to C<sub>2</sub>H<sub>4</sub>, Ag to improve the likelihood of C<sub>2</sub>H<sub>4</sub> epoxidation, or Cu to decrease coke formation.

#### CONCLUSION

The direct conversion of C<sub>2</sub>H<sub>6</sub> and O<sub>2</sub> to produce EO in one step at ambient temperature and atmospheric pressure was studied for the first time in a DBD reactor using two parallel frosted glass plates. The effects of different operating parameters, such as applied voltage, input frequency, and O<sub>2</sub>/C<sub>2</sub>H<sub>6</sub> feed molar ratio, on the EO synthesis performance were also investigated to attain the optimum conditions. The highest EO selectivity of 42.6%, EO yield of 19.4%, and lowest power consumption per EO molecule produced of 6.7 x 10<sup>-18</sup> Ws/molecule were achieved at the optimum applied voltage of 7 kV, input frequency of 550 Hz, and O<sub>2</sub>/C<sub>2</sub>H<sub>6</sub> feed molar ratio of 1:1. Compared to the catalyst-alone system using an Ag catalyst, the studied DBD system was demonstrated to be a potential alternative for the direct conversion of C<sub>2</sub>H<sub>6</sub> to EO, resulting in obviously higher C<sub>2</sub>H<sub>6</sub> conversion, EO selectivity and yield. A DBD system in cooperation with effective catalysts should be investigated further to improve EO selectivity.

#### ACKNOWLEDGMENT

This research was funded by King Mongkut's University of Technology, North Bangkok (Contact no. KMUTNB-64-KNOW-24), and the Office of the Permanent Secretary, Ministry of Higher Education,

Science, Research, and Innovation (Grant No. RGNS 63-087), and supported in part by the Thailand Institute of Nuclear Technology (Public Organization) to the University Program. A special thank you to Material and Process Engineering Technology (MPet), Faculty of Engineering and Technology, KMUTNB, for providing the catalyst preparation equipment.

## REFERENCES

- [1] H. Alzahrani, J. Bravo-Suárez, *J. Catal.* 418 (2023) 225–236. <https://doi.org/10.1016/j.jcat.2023.01.016>.
- [2] G. Boskovic, D. Wolf, A. Brückner, M. Baerns, *J. Catal.* 224 (2004) 187–196. <https://doi.org/10.1016/j.jcat.2004.02.030>.
- [3] A. Talati, M. Haghghi, F. Rahmani, *Adv. Powder Technol.* 27 (2016) 1195–1206. <https://doi.org/10.1016/j.appt.2016.04.003>.
- [4] J.M. Hollis, F.J. Lovas, P.R. Jewell, L.H. Coudert, *Astrophys. J.* 571 (2002) L59. <https://iopscience.iop.org/article/10.1086/341148>.
- [5] T. Salmi, M. Roche, J. Hernández Carucci, K. Eränen, D. Murzin, *Curr. Opin. Chem. Eng.* 1 (2012) 321–327. <https://doi.org/10.1016/j.coche.2012.06.002>.
- [6] S. Dolmaseven, N. Yuksel, M.F. Fellah, *Sens. Actuators, A* 350 (2023) 114109. <https://doi.org/10.1016/j.sna.2022.114109>.
- [7] T. Pu, H. Tian, M.E. Ford, S. Rangarajan, I.E. Wachs, *ACS Catal.* 9 (2019) 10727–10750. <https://doi.org/10.1021/acscatal.9b03443>.
- [8] W. Diao, C.D. DiGiulio, M.T. Schaal, S. Ma, J.R. Monnier, *J. Catal.* 322 (2015) 14–23. <http://dx.doi.org/10.1016/j.jcat.2014.11.007>.
- [9] C.-J. Chen, J.W. Harris, A. Bhan, *Chem. Eur. J.* 24 (2018) 12405–12415. <https://doi.org/10.1002/chem.201801356>.
- [10] A. Alamdari, R. Karimzadeh, S. Abbaszadeh, *Rev. Chem. Eng.* 37 (2021) 481–532. <https://doi.org/10.1515/revce-2017-0109>.
- [11] P.H. Keijzer, J.E. van den Reijen, C.J. Keijzer, K.P. de Jong, P.E. de Jongh, *J. Catal.* 405 (2022) 534–544. <https://doi.org/10.1016/j.jcat.2021.11.016>.
- [12] Y. Wu, A. Yan, Y. He, B. Wu, T. Wu, *Catal. Today* 158 (2010) 258–262. <https://doi.org/10.1016/j.cattod.2010.03.041>.
- [13] J. Gao, D. Zhou, Y. Wu, T. Wu, *Catal. Commun.* 30 (2013) 51–55. <http://dx.doi.org/10.1016/j.catcom.2012.10.023>.
- [14] A. Fridman, A. Gutsol, Y.I. Cho, *Adv. Heat Transfer* 40 (2007) 1–142. [https://doi.org/10.1016/S0065-2717\(07\)40001-6](https://doi.org/10.1016/S0065-2717(07)40001-6).
- [15] D. Li, V. Rohani, F. Fabry, A. Parakkulam Ramaswamy, M. Sennour, L. Fulcheri, *Appl. Catal., B* 261 (2020) 118228. <https://doi.org/10.1016/j.apcatb.2019.118228>.
- [16] Y.P. Zhang, Y. Li, Y. Wang, C.J. Liu, B. Eliasson, *Fuel Process. Technol.* 83 (2003) 101–109. [http://dx.doi.org/10.1016/S0378-3820\(03\)00061-4](http://dx.doi.org/10.1016/S0378-3820(03)00061-4).
- [17] Y. Li, C.J. Liu, B. Eliasson, Y. Wang, *Energy Fuels* 16 (2002) 864–870. <https://doi.org/10.1021/ef0102770>.
- [18] B. Lee, E.S. Jo, I. Heo, T.-H. Kim, D.-W. Park, *Chem. Eng. Process.* 179 (2022) 109070. <https://doi.org/10.1016/j.cep.2022.109070>.
- [19] U.H. Dahiru, F. Saleem, F.T. Al-sudani, K. Zhang, A.P. Harvey, *Chem. Eng. Process.* 178 (2022) 109035. <https://doi.org/10.1016/j.cep.2022.109035>.
- [20] S. Li, Y. Li, X. Yu, X. Dang, X. Liu, L. Cao, *J. Clean. Prod.* 368 (2022) 133073. <https://doi.org/10.1016/j.jclepro.2022.133073>.
- [21] Y. Zhang, H. Zhang, A. Zhang, P. Héroux, Z. Sun, Y. Liu, *Chem. Eng. J.* 458 (2023) 141406. <https://doi.org/10.1016/j.cej.2023.141406>.
- [22] C.A. Aggelopoulos, D. Tataraki, G. Rassias, *Chem. Eng. J.* 347 (2018) 682–694. <https://doi.org/10.1016/j.cej.2018.04.111>.
- [23] J. Sima, J. Wang, J. Song, X. Du, F. Lou, Y. Pan, Q. Huang, C. Lin, Q. Wang, G. Zhao, *Chemosphere* 317 (2023) 137815. <https://doi.org/10.1016/j.chemosphere.2023.137815>. <http://www.ijma.info/index.php/ijma/article/view/1854>.
- [24] T. Sreethawong, T. Suwannabart, S. Chavadej, *Plasma Chem. Plasma Process.* 28 (2008) 629–642. <https://doi.org/10.1007/s11090-008-9149-8>.
- [25] T. Suttikul, S. Yaowapong-aree, H. Sekiguchi, S. Chavadej, J. Chavadej, *Chem. Eng. Process.* 70 (2013) 222–232. <https://doi.org/10.1016/j.cep.2013.03.018>.
- [26] T. Suttikul, B. Paosombat, M. Santikunaporn, M. Leethochawalit, S. Chavadej, *Ind. Eng. Chem.* 53 (2014) 3778–3786. <https://doi.org/10.1021/ie402659c>.
- [27] T. Suttikul, S. Kodama, H. Sekiguchi, S. Chavadej, *Plasma Chem. Plasma Process.* 34 (2014) 187–205. <https://doi.org/10.1007/s11090-013-9492-2>.
- [28] S. Chavadej, W. Dulyalaksananon, T. Suttikul, *Chem. Eng. Process.* 107 (2016) 127–137. <http://dx.doi.org/10.1016/j.cep.2016.05.010>.
- [29] X. Zhang, A. Zhu, X. Li, W. Gong, *Catal. Today* 89 (2004) 97–102. <https://doi.org/10.1016/j.cattod.2003.11.015>.
- [30] F. Cameli, P. Dimitrakellis, G.D. Stefanidis, D.G. Vlachos, *Plasma Chem. Plasma Process.* (2023). <https://doi.org/10.1007/s11090-023-10343-w>.
- [31] T. Suttikul, C. Tongurai, H. Sekiguchi, S. Chavadej, *Plasma Chem. Plasma Process.* 32 (2012) 1169–1188. <https://doi.org/10.1007/s11090-012-9398-4>.
- [32] C. Liu, A. Marafee, B. Hill, G. Xu, R. Mallinson, L. Lobban, *Ind. Eng. Chem.* 35 (1996) 3295–3301. <https://doi.org/10.1021/ie960138j>.
- [33] B.L. Farrell, V.O. Igenegbai, S. Linic, *ACS Catal.* 6 (2016) 4340–4346. <https://doi.org/10.1021/acscatal.6b01087>.
- [34] A.V. da Rosa, J.C. Ordóñez, *Fundamentals of Renewable Energy Processes*, Academic Press, Oxford (2022), pp. 425. <https://doi.org/10.1016/B978-0-12-816036-7.00021-X>.
- [35] J.J. Zou, C.J. Liu, *Carbon Dioxide as Chemical Feedstock*, M. A. Editor Ed., Wiley-VCH, Weinheim (2010), pp. 274–279. <https://doi.org/10.1002/9783527629916.ch10>.
- [36] R. Sanchez-Gonzalez, Y. Kim, L.A. Rosocha, S. Abbate, *IEEE Trans. Plasma Sci.* 35 (2007) 1669–1676. <https://doi.org/10.1109/TPS.2007.910743>.

- [37] Y. Li, G.-h. Xu, C.-j. Liu, B. Eliasson, B.-z. Xue, *Energy Fuels* 15 (2001) 299–302.  
<http://dx.doi.org/10.1021/ef0002445>.
- [38] S. Ahmed, A. Aitani, F. Rahman, A. Al-Dawood, F. Al-Muhaish, *Appl. Catal. A: Gen* 359 (2009) 1–24.  
<https://doi.org/10.1016/j.apcata.2009.02.038>.
- [39] C. De Bie, J. Van Dijk, A. Bogaerts, *J. Phys. Chem. C* 120 (2016) 25210–25224.  
<https://doi.org/10.1021/acs.jpcc.6b07639>.
- [40] D. Ren, G. Cheng, J. Li, J. Li, W. Dai, X. Sun, D. Cheng, *Catal. Lett.* 147 (2017) 2920–2928.  
<https://doi.org/10.1007/s10562-017-2211-5>.
- [41] A. Chongterdtoonskul, J.W. Schwank, S. Chavadej, *J. Mol. Catal.* 372 (2013) 175–182.  
<http://dx.doi.org/10.1016/j.molcata.2013.02.016>.

THITIPORN SUTTIKUL<sup>1,2</sup>  
SIRIMAS MANTHUNG<sup>1</sup>  
SASIKARN NUCHDANG<sup>3</sup>  
DUSSADEE RATTANAPHRA<sup>3</sup>  
THONGCHAI PHOTSATHIAN<sup>4</sup>

<sup>1</sup>Division of Chemical Process Engineering Technology, Faculty of Engineering and Technology, King Mongkut's University of Technology North Bangkok, Rayong, Thailand

<sup>2</sup>The Plasma and Automatic Electric Technology Research Group, King Mongkut's University of Technology North Bangkok, Rayong, Thailand

<sup>3</sup>Research and Development Division, Thailand Institute of Nuclear Technology, Pathum Thani, Thailand

<sup>4</sup>Division of Instrumentation and Automation Engineering Technology, Faculty of Engineering and Technology, King Mongkut's University of Technology North Bangkok, Rayong, Thailand

## JEDNOSTEPENA KONVERZIJA ETANA U ETILEN-OKSID U DIELEKTRIČNOM BARIJERNOM PRAZNIJENJU PARALELNIH PLOČA

*U ovom radu je proučavana konverzija etana (C<sub>2</sub>H<sub>6</sub>) u etilen oksid (EO) u jednom koraku u sistemu dielektričnog barijernog pražnjenja (DBP) sa dve paralelne mat staklene ploče na temperaturi okoline i atmosferskom pritisku. EO se direktno proizvodi iz etana u jednom koraku bez potrebe za odvajanjem i recikliranjem etilena. Ispitivani su efekti primenjenog napona, ulazne frekvencije i molskog odnosa O<sub>2</sub>/C<sub>2</sub>H<sub>6</sub> napojne smeše na performanse sinteze EO. Rezultati su pokazali da su veći primenjeni napon i niža ulazna frekvencija generisali više energetskih elektrona, što je rezultiralo većom strujom. Više elektrona se sudarilo sa molekulima gasa reaktanta da bi pokrenuli plazma reakcije, povećavajući konverzije C<sub>2</sub>H<sub>6</sub> i O<sub>2</sub>. Povećani molski odnos O<sub>2</sub>/C<sub>2</sub>H<sub>6</sub> dovode poboljšao je konverziju C<sub>2</sub>H<sub>6</sub> i O<sub>2</sub>. Utvrđeno je da su optimalni uslovi primenjeni napon od 7 kV, ulazna frekvencija od 550 Hz i molski odnos O<sub>2</sub>/C<sub>2</sub>H<sub>6</sub> od 1:1, koji je pokazao najveću selektivnost EO (42,6%), prinos EO (19,4%), i najmanja potrošnja energije po proizvedenom EO (6,7 x 10<sup>-18</sup> Ws/molekul).*

*Ključne reči: dielektrično barijerno pražnjenje, epoksidacija, oksidativna dehidrogenacija etilen oksida, jednostepena reakcija.*